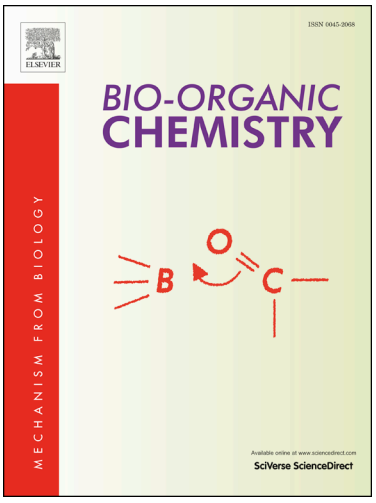

Dihydroactinidiolide, a natural product against $A\beta_{25-35}$ induced toxicity in Neuro2A cells: Synthesis, *in silico* and *in vitro* studies

Mamali Das, Sengodu Prakash, Chirasmita Nayak, Nandhini Thangavel, Sanjeev Kumar Singh, Paramasivam Manisankar, Kasi Pandima Devi

PII: S0045-2068(18)30600-X
DOI: https://doi.org/10.1016/j.bioorg.2018.08.037
Reference: YBIOO 2494

To appear in: *Bioorganic Chemistry*

Received Date: 18 June 2018
Revised Date: 24 August 2018
Accepted Date: 27 August 2018

Please cite this article as: M. Das, S. Prakash, C. Nayak, N. Thangavel, S. Kumar Singh, P. Manisankar, K. Pandima Devi, Dihydroactinidiolide, a natural product against $A\beta_{25-35}$ induced toxicity in Neuro2A cells: Synthesis, *in silico* and *in vitro* studies, *Bioorganic Chemistry* (2018), doi: https://doi.org/10.1016/j.bioorg.2018.08.037

Dihydroactinidiolide, a natural product against $A\beta_{25-35}$ induced toxicity in Neuro2A cells: Synthesis, *in silico* and *in vitro* studies

Mamali Das[1], Sengodu Prakash[2], Chirasmita Nayak[3], Nandhini Thangavel[1], Sanjeev Kumar Singh[3], Paramasivam Manisankar[2], Kasi Pandima Devi[1]*

[1] Department of Biotechnology, Alagappa University, Karaikudi-630003, India.

[2] Department of Industrial Chemistry, Alagappa University, Karaikudi-630003, India.

[3] Department of Bioinformatics, Alagappa University, Karaikudi-630003, India.

* **Correspondence:**

Kasi Pandima Devi

Email: devikasi@yahoo.com

Keywords: Dihydroactinidiolide; Acetylcholinesterase; Alzheimer's disease; ADME; Amyloid $\beta_{25-35;}$ Neuro2a cells.

ABSRACT

Synthesis of natural products has speeded up drug discovery process by minimizing the time for their purification from natural source. Several diseases like Alzheimer disease (AD) demand exploring multi targeted drug candidates, and for the first time we report the inhibitory potential of a novel anti AD target, which is the synthesized dihydroactinidiolide (DA). Though the activity of DA containing solvent extracts have been proved to possess free radical scavenging, anti bacterial and anti cancer activities, the pharmacological properties of DA per se has not been evidenced yet. Hence DA was successfully synthesized from β-ionone using facile two-step oxidation method. It showed potent acetylcholinesterase (AChE) inhibition with half maximal inhibitory concentration (IC_{50}) 34.03nM, which was further supported by molecular docking results showing strong H bonding with some of the active site residues such as GLY117, GLY119 and SER200 of AChE. Further it displayed DPPH and (.NO) scavenging activity with IC_{50} value

50nM and metal chelating activity with IC_{50} >270nM. Besides, it significantly prevented amyloid β_{25-35} self-aggregation and promoted its disaggregation at 270nM. It did not show cytotoxic effect towards N2a cells up to 24 hr at 50 and 270nM while it significantly increased viability of amyloid β_{25-35} treated N2a cells through ROS generation at both the concentrations. Cytotoxicity profile of DA against human PBMC was quite impressive. Hemolysis studies also revealed very low hemolysis i.e. minimum 2.35 to maximum 5.61%. It also had suitable ADME properties which proved its druglikeness. The current findings demand for further *in vitro* and *in vivo* studies to develop DA as a multi target lead against AD.

1. Introduction

Natural products remained as an inseparable part of human civilization from time immemorial with proven effect against numerous deadly diseases like cancer, cardiovascular and many more. Though they represent a very minute quantity in natural source their successful synthesis from commercially available compounds has been exploited immensely to test them individually for specific disease related pathologies. Dihydroactinidiolide (DA), a structural analog of loliolide and degradation product of carotenoids [1],[2] that has been found to be responsible for the aroma of black tea and tobacco [3],[4]. It is a potent plant growth inhibitor, a regulator of gene expression and is responsible for photo acclimation in Arabidopsis [5],[6]. Furthermore it is a component of queen recognition pheromone of *Solenopsis invicta* [7] and was first isolated from *Actinidia polygama* as an attractant for Felidae family [8]. Most of the studies involving DA has been carried out in extract form such as DA present in methylene chloride extract of *Prosopis farcta* showed free radical scavenging antioxidant activity and anticancer activity against four human tumor cell lines like Epitheliod carcinoma (Hela), human prostate cancer (PC3), mammary gland breast cancer (MCF-7) and hepatocellular carcinoma (HePG-2) [9]. Further DA

identified in *Cladophora fascicularis* showed antibacterial activity [10]. In the current study, we have synthesized DA to verify its individual neuroprotective effect. The first report of its synthesis was through photosensitized oxidation of β-ionone [11]. Subsequently its synthesis has been reported from (S)-3-hydroxy- 2,2-dimethylcyclohexanone, tert-hydroxyolefins, 2,6 dimethylcyclohexanone, (S)-2,4,4-trimethyl-2-cyclohexen-1-ol, 2,6,6-trimethyl-1-cyclohexene-1-acetaldehyde, 2,6,6-trimethylcylohexenone, 1,3,3-trimethylcyclohexene and β-ionone [12-19] while to the best of our knowledge there is no subsequent studies on biological activity screening, particularly on neuroprotective reports of the synthesized DA.

Alzheimer's disease (AD), the sixth leading cause of worldwide dementia is a progressive neurodegenerative disorder, with complicated interaction of biochemical and genetic factors, contributing to severe cognitive decline. In this regard acetylcholinesterase inhibitors (AChEIs) have been used for a decade [20]. Despite of huge clinical practice, the efficacy of AChEIs like donepezil has been questioned as they improve cognitive and behavioral symptoms and do not prevent neurodegeneration [21]. On the other hand multiple AD etiology provide credence that a more successful approach will be a single natural product based compound with the ability to interact with several molecular targets involved in AD [22-24]. Commercial anti AD drugs such as tacrine, revastigmine, donepezil and galantamine not only provide symptomatic benefits [25] but also show deleterious side effects. Recently our group [26],[27], and many other researchers [28-31] reported neuroprotective effect of a number of plants and algal extracts. However none of them have explained for specific leads responsible of anti AD effect of the extract which may be due to the tedious procedure associated with isolation and purification of leads. Hence present study was designed to synthesize DA and analyze its neuroprotective effect using both *in silico* and *in vitro* methods.

2. Material and Methods

2.1. Chemistry

Reagents and solvents were obtained commercially and used as received. NMR data was recorded on a BRUKER Advance 500 MHz spectrometer 1H and ^{13}C-NMR using deuterochloroform ($CDCl_3$) as solvent and tetramethylsilane (TMS) as internal standard. Elemental analysis was measured by means of Perkin Elmer 2400 CHN elemental analyzer flowchart.

2.2. Synthesis

DA was synthesized by protocol followed by previous report of [32]. In briefly, 1 mole of β-Ionone (Alfa Aesar, 96%) and 2 moles of *m*-chloroperoxybenzoic acid (SRL, pure 55-75%) was dissolved in 10 mL of dichloromethane (DCM). The mixture was maintained at 2-5°C for 24 h with continuous stirring **(Scheme 1)**.

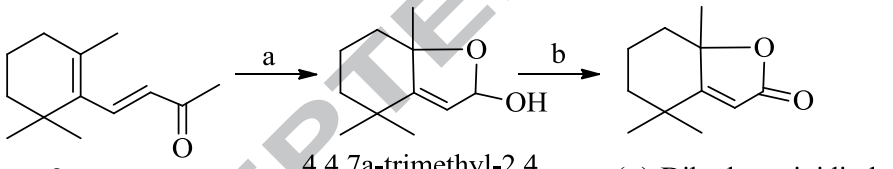

β-Ionone

4,4,7a-trimethyl-2,4, 5,6,7,7a-hexa hydro benzofuran-2-ol

(±)-Dihydroactinidiode

Conditions: (a) m-Chloroperoxybenzoic acid, 2-5°C, dichloromethane; (b) Anhydrous chromic trioxide in acidic medium.

Scheme 1 Synthesis of dihydroactinidiolide from β-ionone by two-step oxidation method.

The product was purified by adding sodium thiosulfate to remove excess of acid. The product was subsequently subjected to alkaline hydrolysis to obtain benzofuranol which was further oxidized with chromic anhydride to DA that has purification by flash chromatography (CH_2Cl_2/MeOH 15:1) yielded DA (220 mg, 85%) as a waxy solid. The products obtained were

characterized by spectroscopic methods such as FTIR, ^{1}H NMR, ^{13}C NMR and elemental analysis and have been matched by previously reported samples [26]. ^{1}H NMR (500 MHz, DMSO-d_6), δ 5.75 (s, 1H, CH, alkenes), 1.65 (m, 2H, CH_2), 1.50 (s, 3H, CH_3), 1.37 (m, 1H, CH_2), 1.35 (m, 1H, CH_2), 1.22 (s, 3H, CH_3), and 1.18 (s, 3H, CH_3). ^{13}C NMR (500 MHz, DMSO-d_6), δ 19.5, 23.3, 23.2, 29.6, 37.3, 40.6, 41.4, 86.6, 112.3, 172.0, and 182.8. Anal. Calcd for $C_{35}H_{54}O_5$: C, 75.77; H, 9.81; O, 14.42. Found: C, 75.71; H, 9.90; O, 14.41.

2.3 Acetylcholinesterase inhibitory assay

AChE inhibitory activity of DA was measured using the method of Ellman [33]. Briefly 10μL of 0.1U enzyme and 5.5–55nM of DA were incubated and allowed to react for 45 min in a 96-well plate. The reaction was stopped by the addition of 50mM Tris-HCl pH 8.0. To this mixture, 125μL of 3mM DTNB and 50μL of 15mM substrate were added to initiate the reaction. The absorbance was taken at 405 nm and the % inhibition was calculated as follows. The IC_{50} value was calculated using GraphPad Prism Software (version 3.02, GraphPad Software Inc., San Diego, CA).

$$\%\ \text{of AChE lnhibition} = \frac{\text{Specific activity of control} - \text{specific activity of test}}{\text{Specific activity of control}} \times 100$$

2.4 DPPH radical scavenging assay

DPPH radical scavenging activity of DA was measured using the method developed by Blois [34]. DPPH (0.1mM) was added to different concentrations of DA (50-270nM) and the reaction mixture was allowed to react in the dark for 30 min. The absorbance was measured at 517 nm. BHT (40–220nM) was used as the standard.

$$\%\ \text{DPPH Scavenging} = \frac{\text{Absorbance of test} - \text{Absorbance of control}}{\text{Absorbance of control}} \times 100$$

2.5 Nitric oxide radical scavenging activity

Nitric oxide radical scavenging activity of DA was determined by Griess reaction [35]. Reaction mixture containing 10mM sodium nitroprusside in phosphate-buffered saline (pH 7.4) and DA (50-270nM) were incubated at 25 °C for 150 min. To this reaction mixture, Griess reagent (1% sulphanilamide in 5% orthophosphoric acid and 0.1% naphthyl ethylenediamine in distilled water) was added. The solution was mixed and allowed to stand for 10 min at 25 °C and the absorbance was measured at 546 nm. BHT (40–220nM) was used as the standard.

$$\%\ (.\mathrm{NO})\ \text{Scavenging} = \frac{\text{Absorbance of test} - \text{Absorbance of control}}{\text{Absorbance of control}} \times 100$$

2.6 Metal chelating activity

Metal chelating activity of DA was determined followed by Dinis [36]. Briefly DA of concentrations 50-270nM were added to a solution of 0.15mM FeSO4 and reaction was initiated by 5mM ferrozine. The mixture was kept at room temperature for 10 min. Absorbance of the mixture was measured at 562nm against the blank performed in the same way. BHT (30-170nM) served as the positive control while sample without DA served as negative control. The rate of inhibition of Fe^{2+}-ferrozine complex formation was calculated as follows

$$\%\ \text{of inhibition} = \frac{\text{Absorbance of test} - \text{Absorbance of control}}{\text{Absorbance of control}} \times 100$$

2.7 Amyloid β25–35 anti aggregation and disaggregation assays

The anti-aggregation and disaggregation property of the synthesized compound was evaluated in two phases [37]. In phase I, oligomers were used to check the inhibition of aggregate formation then in Phase II the disaggregation of the pre-formed fibrils were determined. Freshly prepared $A\beta_{25-35}$ (100μM) monomers were incubated in Tris-HCl buffer pH 7.4 at 37°C for 24 h. DA (50 and 270nM) was added to the oligomers and incubated for 48 h. The $A\beta_{25-35}$ oligomers were incubated with/without DA for 24 h, 48 h, 96 h and 9 days. The

aggregation pattern was evaluated by ThT assay with the aliquots taken from the incubation mixture at 24 h and 48 h. DA was co-incubated with the pre-formed fibrils, and the disaggregation pattern was evaluated by taking the aliquots of 96 h and 9 days by Thioflavin T assay using Galanthamine (50μM) as standard.

2.8 Thioflavin T assay

Amyloid fibril formation was measured by Thioflavin T assay. Aliquots (10μl) from the incubation mixtures of both the phases were added to 50mM glycine—NaOH buffer (pH 8.5) containing 5mM Thioflavin T. Each sample was analyzed in triplicates and the fluorescence intensities were measured at 450nm (excitation) and 485nm (emission) under time resolved fluorescence mode in Spectramax M3 reader (Molecular Devices). The background fluorescence emitted by ThT was subtracted from the values of all the samples.

2.9 Microfluorescence assay

About 5 μl aliquot of the fibrillated $A\beta_{25-35}$ peptide (100μM) sample was diluted (1:2) with 5μM ThT in 50mM glycine-NaOH buffer (pH 8.5) and transferred onto a slide. Fluorescent signals (488nm) were then visualized by the Confocal Laser Microscope System (CLSM FV300, Olympus, Tokyo, Japan).

2.10 Cytotoxicity of DA and donepezil on N2a Cells

Neuro2a (N2a) cell line was obtained from the Centre for cellular and Molecular Biology, Hyderabad and maintained routinely in Dulbecco's Modified Eagle Medium at 37°C in a humidified atmosphere in the presence of 5% CO_2 in poly-D-lysine-coated T-25 flasks. To examine neuronal cell toxicity, N2a cells were exposed to DA and donepezil for 24 h at 50–270nM concentrations, and cell viability was measured by 3-(4,5-

dimethylthiazol-2-yl)-2,5-diphenyl tetrazolium bromide (MTT) assay by the following formula.

% of cell viability = (Absorbance of test/Absorbance of control)×100

2.11 Effect of $A\beta_{25-35}$ on DA treated N2a cells

N2a cells (2×10^5/ml) were pre-treated with different concentrations of DA (50–270nM) and donepezil (50μM) for 2 hour, and exposed to 20μM of $A\beta_{25-35}$ for 24 hour the cell viability was assessed by MTT assay.

2.12 Measurement of intracellular ROS

N2a cells (2×10^5/ml) were pre incubated with DA (50–270nM) and donepezil (50μM) for 2 hour, and exposed to 20μM of $A\beta_{25-35}$ for 24 hour and cells were incubated with 10 μM DCFH-DA for 30 min at 37°C in darkness and treated with lysis buffer. The intensity of fluorescence was determined using a multilabel reader (Molecular Device Spectramax M3, equipped with Softmax Pro V5 5.4.1 software) with the excitation and emission wavelength of 485 and 535 nm. The results are expressed as fluorescent intensity of DCF (AU).

2.13 In vitro cytotoxicity assay using PBMC

Whole blood from healthy volunteers was collected into EDTA coated tubes and was diluted with equal volume (3ml) of RPMI medium (Himedia, India). Peripheral blood mononuclear cells (PBMC) were separated by density gradient centrifugation at 400 g using Lymphocyte separation medium, (Himedia, India). The white layer formed intermittently was taken and washed with RPMI 1640 and centrifuged at 200 g for 10 min, the pellet was suspended in RPMI medium (with 10% sterile bovine serum (FBS) and 1X antibiotics) and checked for viability by MTT assay. Then PBMC was treated with different concentration of DA and after 24 hr washed with PBS and treated with 1 ml of fresh medium containing 1 mg/ml of MTT and

were incubated for 3 h at 37°C in dark. The violet MTT formazan product formed was dissolved in DMSO and the absorbance was determined at 570nm by a spectrophotometer. The results are represented as percentage of viable cells compared with the control. 1mM H_2O_2 was used as the positive control. The morphology and integrity of the cell membrane of PBMC was assessed by under a light microscope.

2.14 Hemolytic activity

Hemolytic activity of DA was determined as explained by [38]. Blood from healthy human volunteers were collected in heparinized tubes and centrifuged at 1500 rpm for 10 min. The pellet was washed thrice with cold PBS pH 7.4 and resuspended in the same buffer. Different doses of DA (50–270nM) were added to the erythrocyte suspension and incubated for 1 h at 37°C in a shaking water bath. After the incubation period, cells were centrifuged and the amount of hemoglobin liberated was quantified in the supernatant by measuring the absorbance at 540nm.

$$Hemolysis\ (\%) = \frac{HbAbs}{Hb100\%Abs} \times 100$$

2.15 Statistical analysis

Statistical analysis was performed using SPSS 17.0 software package. The results of all the experiments were represented as mean ± SD of triplicates employed. Analysis of variance was performed by one-way ANOVA. Significant differences between control and treated groups were determined by Duncan's multiple range tests and p value < 0.05 was regarded as significant.

2.16 Molecular Docking

Molecular docking was used to validate the cell free studies. Lamarckian genetic algorithm methodology was employed for docking by AutoDock 4.2. The standard docking procedure was

followed for a rigid protein and a flexible ligand. A grid of 60, 60, and 60 points in x, y, and z directions was built with a grid spacing of 0.375 Å and a distance-dependent function of the dielectric constant was used for the calculation of the energetic map. The default settings were used for all other parameters.

2.17 Ligand Preparation

3D (.sdf) structure of DA and γ-butyrolactone were downloaded from PubChem (https://pubchem.ncbi.nlm.nih.gov) and converted to its pdb form with the help of online SMILES translator tool.

2.18 Protein preparation and docking procedure

The 3D structure of acetylcholinesterase (1EVE) was selected on the basis of literature survey and downloaded from PDB. The structure was then refined using Autodock software and DiscoveryStudioVisualizer. Grid centers were placed on the active sites which were obtained by online active site prediction tool http://www.scfbio-iitd.res.in/dock/ActiveSite_new.jsp. The GALS method was adopted to perform the molecular docking. The parameters for GA were defined as maximum number of 250,000 energy evaluations. The number of docking runs was set to 100. After docking, all structures generated were assigned to clusters based on a tolerance of 1Å all atoms RMSD from the lowest-energy structure. The results obtained were analyzed using PyMol.

2.19 Molecular dynamics simulation

The crystal structure of Aβ peptide (1QCM) was downloaded from protein Data bank. Molecular dynamics simulation was performed for both with and without DA using Desmond to understand the mechanical insight of assembly of Aβ peptides using Optimized Potentials for Liquid Simulations (OPLS) 2005 force field. Six copies of Aβ peptides were placed randomly

and soaked TIP3P water inside the orthogonal box extending 10Å from any atoms of the protein and DA complex to avoid direct interaction with its own periodic image. The system was neutralized using appropriate NA/CL and 0.15M of salt concentration. Each simulation was subjected to energy minimization using steepest descent algorithm until a gradient threshold (25 kcal/mol/Å) is reached. The equilibration was performed using NVT (constant number, volume and temperature) and NVT (constant number, volume and temperature) to maintain temperature (300 K) and pressure (1 atm). The equilibrated systems were further carried to perform MD simulations for 100 ns at constant temperature and pressure with a time step of 2 fs.

2.20 ADME Profiling using QikProp and SwissADME

The QikProp program was used to predict the essential principle descriptors and physiochemical characteristics of DA which determined its ADME properties. SwissADME (http://www.swissadme.ch/) was used to identify CytP450 inhibitory potential of DA.

3. Results and Discussion

3.1 Chemistry

Scheme 1 shows the synthesis of dihydroactinidiolide through two-step oxidation method as described by Sachihiko et al, 1968. In first step, the β-ionone was oxidized by peroxybenzoicacid, subsequently hydrolysed to obtain benzofuranol derivative. Then, chromic anhydride in strong acidic media was used as catalyst for next oxidation step to receive the target compound.

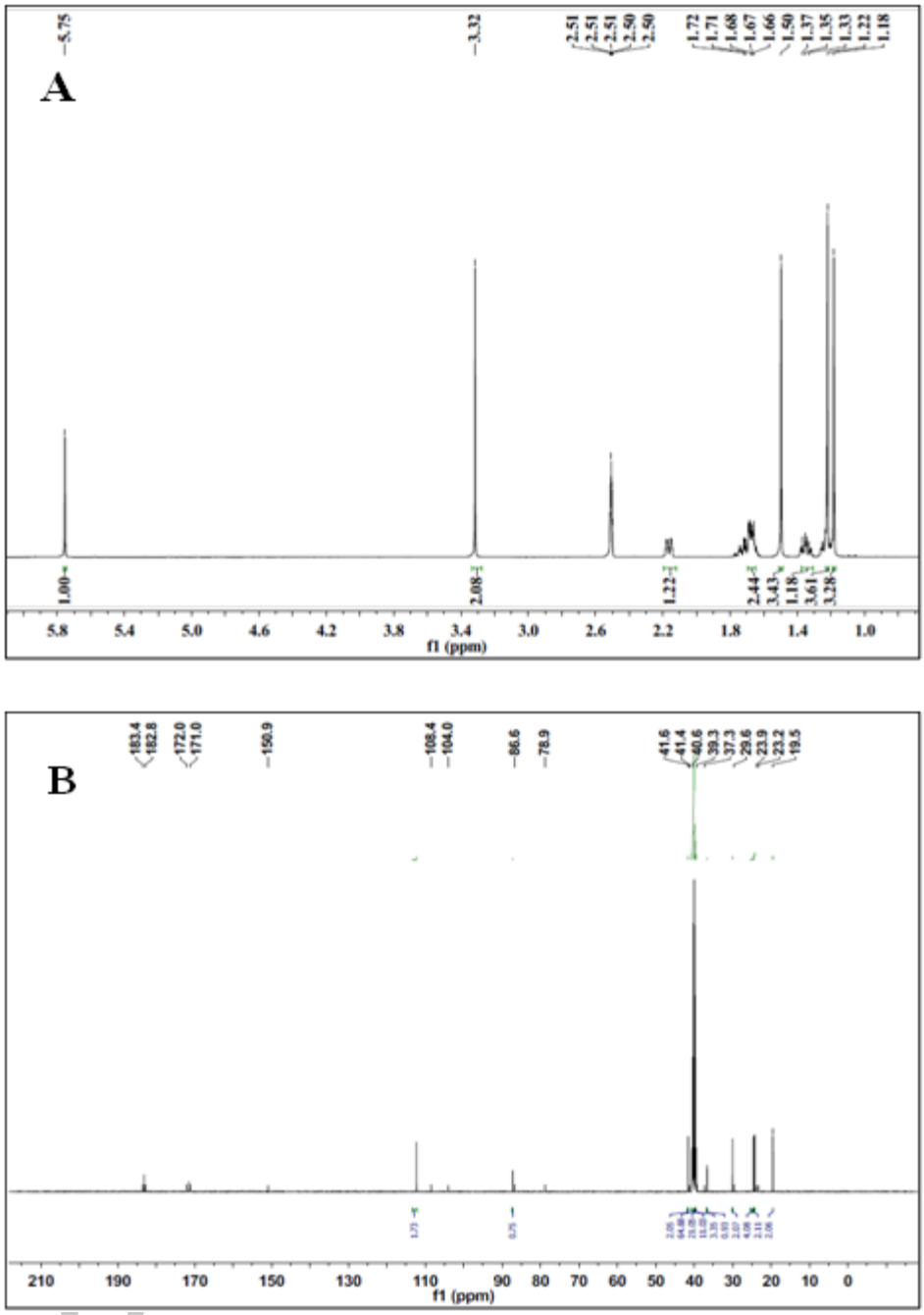

Fig. 1: (A) ^{1}H NMR and (B) ^{13}C NMR at 500 MHz using solvent of DMSO-d_6 of DA.

The chemical structure of the synthesized DA was confirmed spectroscopically. In the ^{1}H NMR spectrum of DA (**Fig. 1A**), the three protons of the methyl group in the cyclohexane ring gave a singlet at 1.22 ppm (3H, s) and 1.18(3H, s). Other methyl group proton was in the two rings at 1.50 ppm (3 H, s). All methylene proton of ring appeared at 1.65 ppm (3 H, bm), 1.35 ppm (1 H, t of d) and 1.37 ppm (1 H, t of d). One alkene proton of furanone ring gave signal at 5.75 ppm (1 H, s). Moreover in ^{13}C-NMR (**Fig. 1B**), cyclohexane like methylene carbon appeared at 40.6 ppm, 19.5 ppm, 41.7 ppm and cyclohexane like carbon signal at 36.5 ppm, 86.6 ppm. 1-carboxyl carbon and 1-ethylene carbon showed at 172.0 ppm and 182.8 ppm, respectively. Cyclohexane like methyl carbon signal appeared at 23.3 ppm, 23.2 ppm, 29.6 ppm.

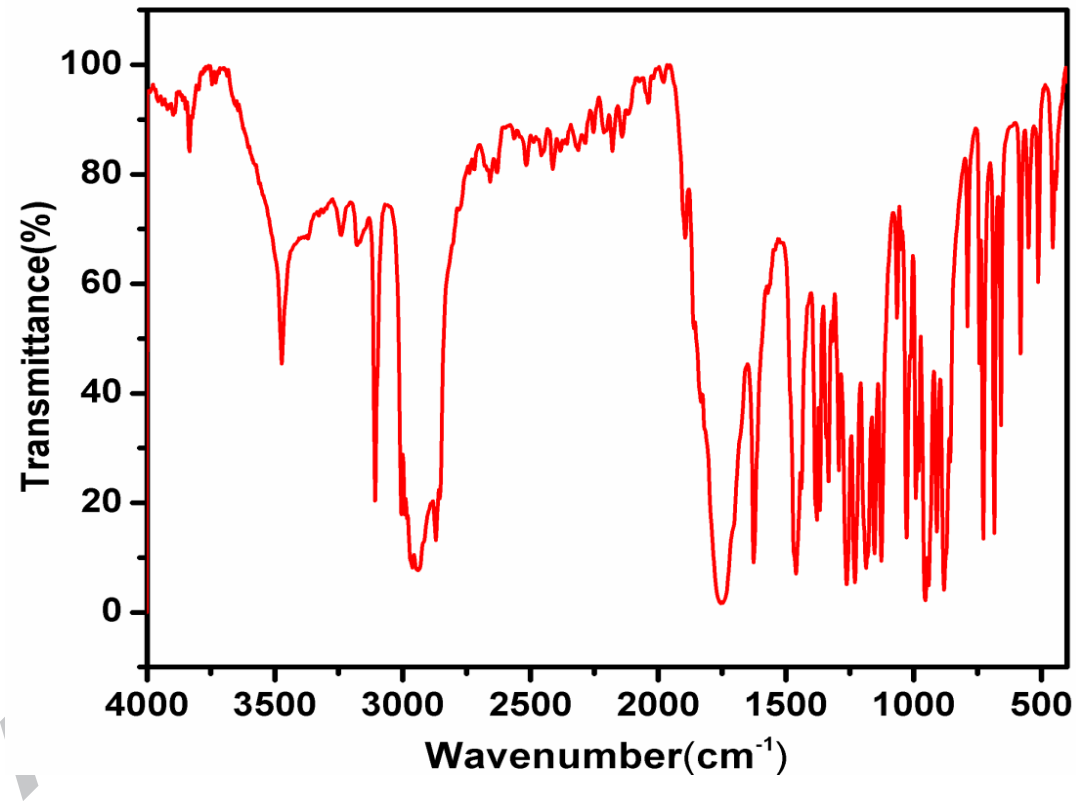

Fig. 2 FTIR of synthesized DA.

Fig. 2 shows the FTIR spectrum of synthesized DA, the important functional group of synthesized compound has been described. A synthesized compound of C=Ostr of appears at

1754 cm^{-1}. A band at 1262 cm^{-1} and 1625 cm^{-1} represented for C-O-C_{str} and C=C_{str}, respectively. A band at 3107 cm^{-1} and 2939 cm^{-1} found for C-H_{str} and =C-H_{str}, respectively.

3.2 Biology

In this work for the first time we report the synthesized DA with significant cell free AChE inhibitory efficiency **(Fig. 3A)** with an IC_{50} 34.03 nM, which was better than recent studies carried out with β-carboline derivatives [39] with IC_{50} values of 0.11-0.76μM and tacrine-1,2,3-

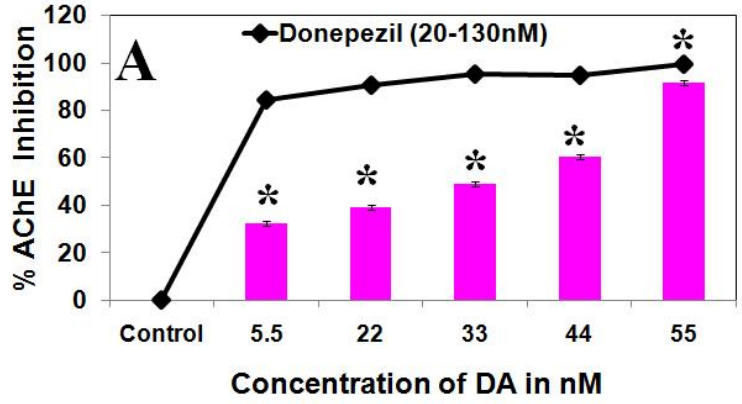

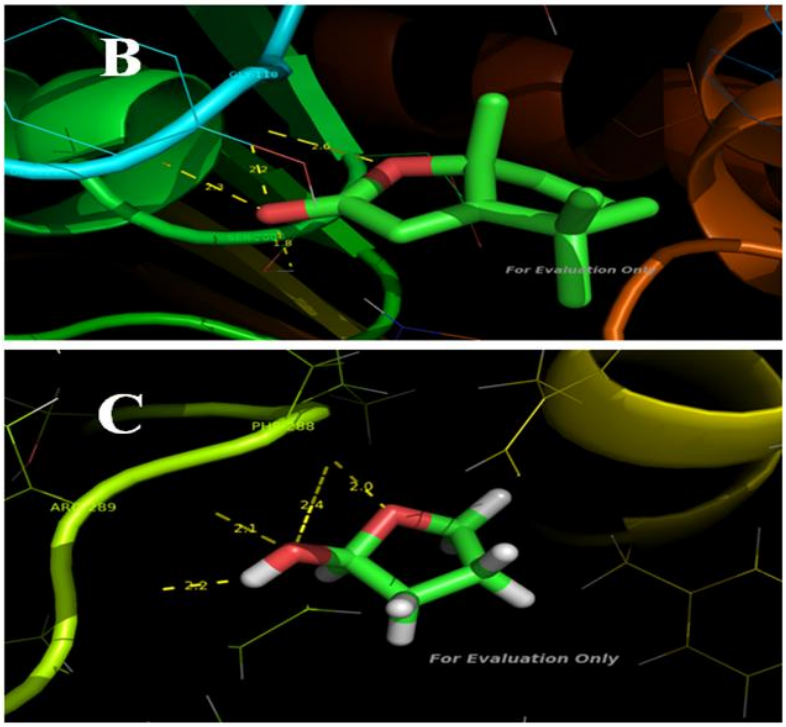

Fig. 3 (A) Acetylcholinesterase inhibitory activity of DA and (B) and (C) PyMol image of DA and γ-butyrolactone binding with AChE active site residues. *Significant level at $p<0.05$ (control versus treated).

triazole derivatives [40] with that of 4.89μM.

This result was further clarified by molecular docking studies where it formed 4 H bonds with three of the active site residues such as GLY118, GLY119 and SER200 **(Fig. 3B)** which were reported to be actively involved in H bonding with several potential inhibitors through molecular dynamics simulation studies [41]. In order to find the structure activity relationship of DA a docking study was carried out with γ-butyrolactone which is found to increase acetylcholine in the cerebral cortex in mice and rats and a common precursor of γ-hydroxybutyrate that occurs naturally in the human brain and acts as a neurotransmitter and neuromodulator [42]. Interestingly it was found to form 4 H bonds with some of the active sites of AchE like PHE288 and ARG289 through its O and H groups **(Fig. 3C)**. This confirms strong H bonding ability of DA which possesses two O groups.

DA showed significant DPPH and (.NO) scavenging activity with IC_{50} <50nM and metal chelating activity with IC_{50} value >270nM **(Fig. 4A, B and C).** Though DA along with 25 other components from petroleum ether fraction of *Grateloupia livida* had significant antioxidant, antibacterial and anti-schistosomal activities [43],[44], the synthesized DA with the aforesaid activities were the first to be reported. Further in recent studies synthesized thiosemicarbazones displayed (.NO) scavenging activity with IC_{50} values 8.6-10.2μM and AChE inhibitory activity with IC_{50} values 1.98-14.26μM [45] which was very high when compared to DA while synthesized N-methylenebenzenamine derivatives had AChE inhibitory potential with IC_{50} values 0.82-25.53μM. This proved its multi target inhibitory efficiency.

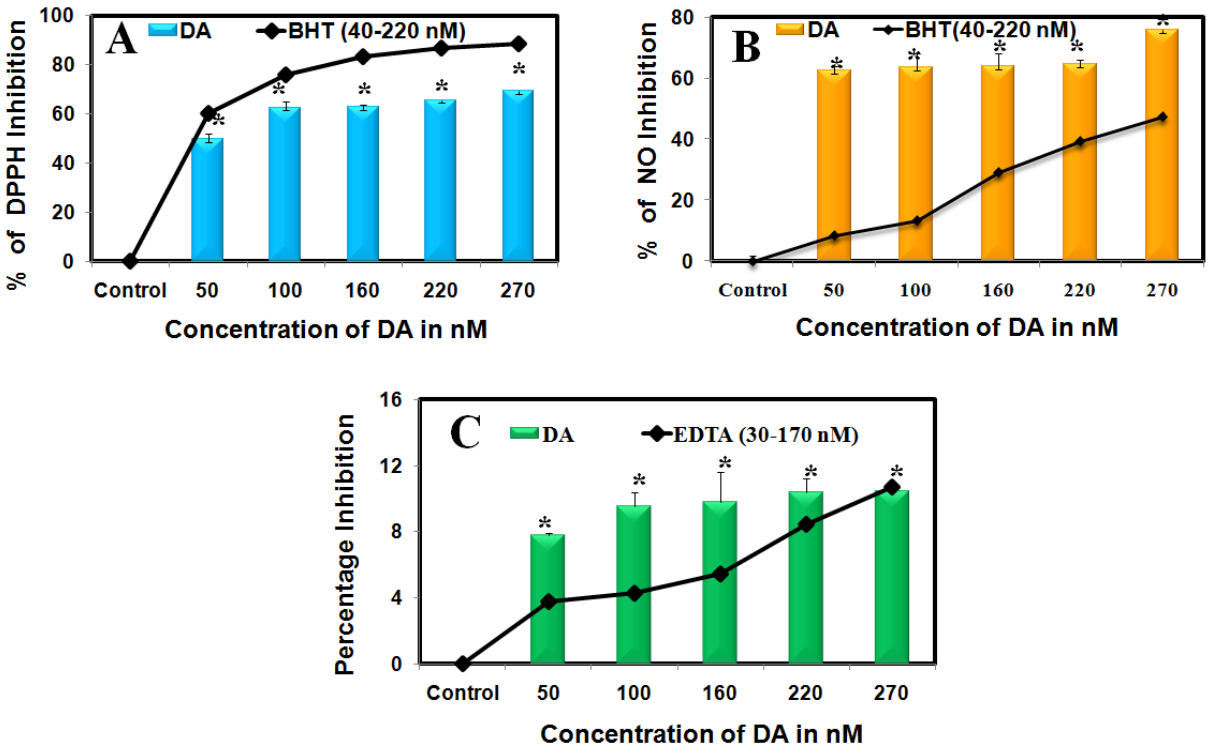

Fig. 4 (A) DPPH radical scavenging, (B) (.NO) radical scavenging and (C) metal chelating activity of DA. *Significant level at $p<0.05$ (control versus treated).

Toxic Aβ aggregation and deposition make a strong obstacle in drug development against AD. In our study, we have used the shortest fragment $A\beta_{25-35}$ for aggregation studies, since it is almost similar in behaviour, aggregation pattern and toxicity when compared with the $A\beta_{1-42}$ peptide [46]. Th-T assay and confocal microscopy revealed antiaggregation and disaggregation potential of DA at 270nM concentration **(Fig. 5A and C)** which is again reported for the first time. In docking studies DA was found to form H bond with LYS28 residue with binding energy of -3.62Kcal/mol **(Fig. 5B)** which has long been recognized as an anchoring residue for membrane phospholipids [47].

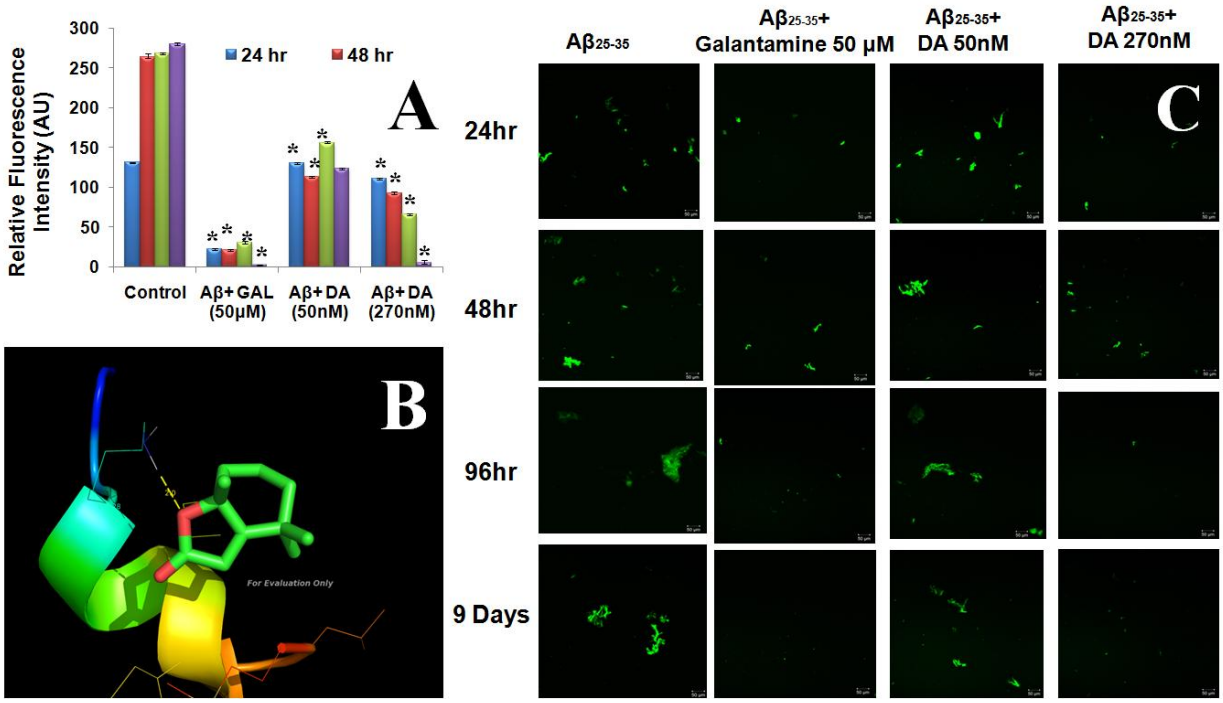

Fig. 5 (A) Effect of different concentrations of DA on aggregation and disaggregation of $A\beta_{25-35}$ in different time intervals, (B) PyMol image of DA biding to $A\beta_{25-35}$ and (C) CLSM images of $A\beta_{25-35}$ treated with different doses of DA in different time intervals. *Significant level at $p<0.05$ (control versus treated).

Therefore DA has been confirmed to inhibit Aβ attachment on the neuronal membrane thereby reducing its aggregation. Further a conformational modification from an α-helix to a β-sheet leading to Aβ oligomerization and fibrilization requires formation of a salt bridge between Asp 23 or Glu 22 and Lys 28. Recently, Cu^{2+} and galanthamine have been reported to inhibit the formation of Aβ fibrils through Glu 22 and Asp 23 or Lys 28 [48]. This suggests DA can therefore be used to prevent formation of β turn and thus the formation of Aβ fibrils. Molecular dynamics simulation revealed that in the absence of DA, all the Aβ peptides started aggregating from 10ns and remained intact throughout the simulation time period **(Fig. 6A and B)**, while in the presence of DA, Aβ peptide has not been aggregated during the simulation period, which was

in agreement with CLSM and ThT data.

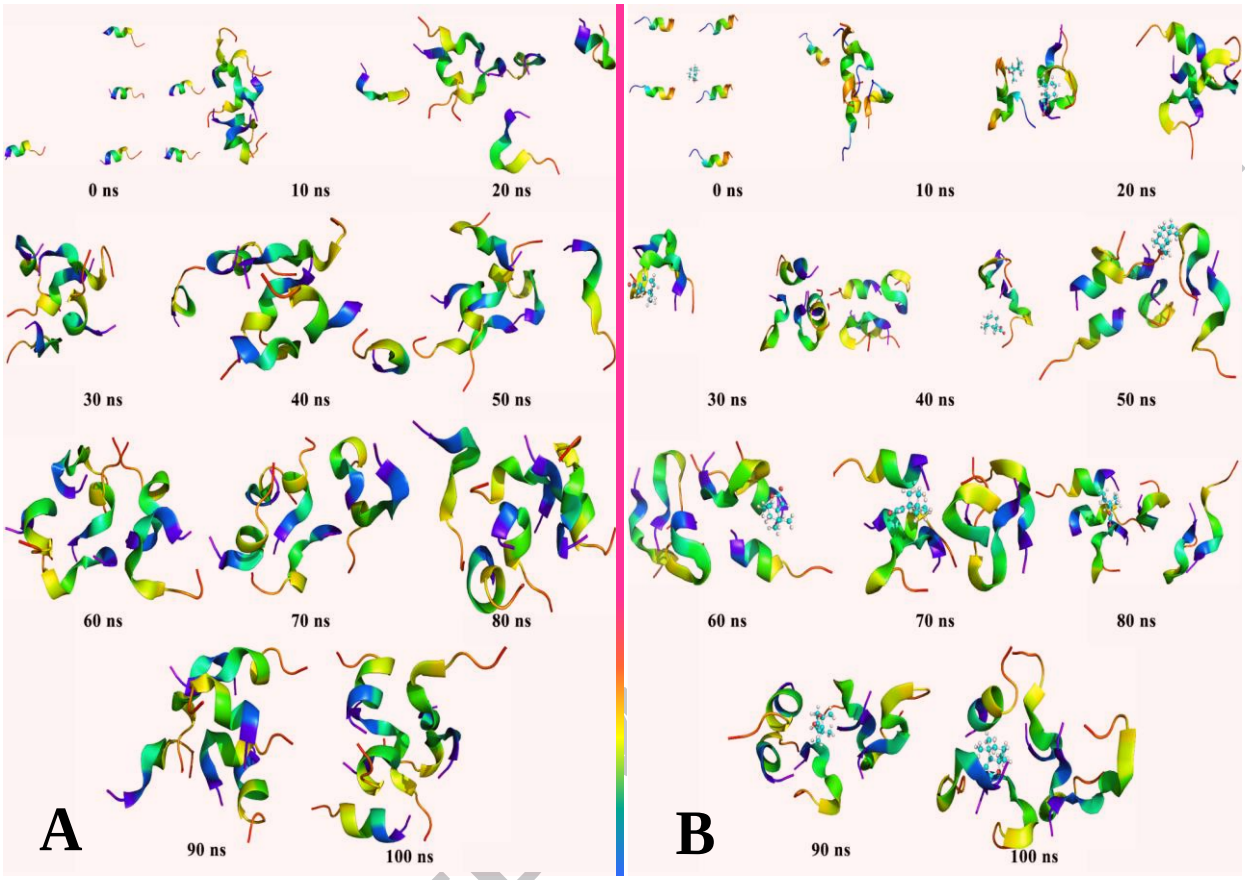

Fig. 6 (A) Aggregation of $A\beta_{25-35}$ in absence and (B) presence of DA.

Further we have checked the effect of different concentrations of DA on viability of N2a cells by MTT assay and compared it with the standard drug donepezil **(Fig. 7)**. Here we found that DA and donepezil had similar effect on N2a cell viability. Similarly $A\beta_{25-35}$ treatment has significantly decreased the cell viability at 24 h when compared to the control cells and DA has significantly increased viability of $A\beta_{25-35}$ treated N2a cells at both 50 and 270nM when compared to the standard donepezil.

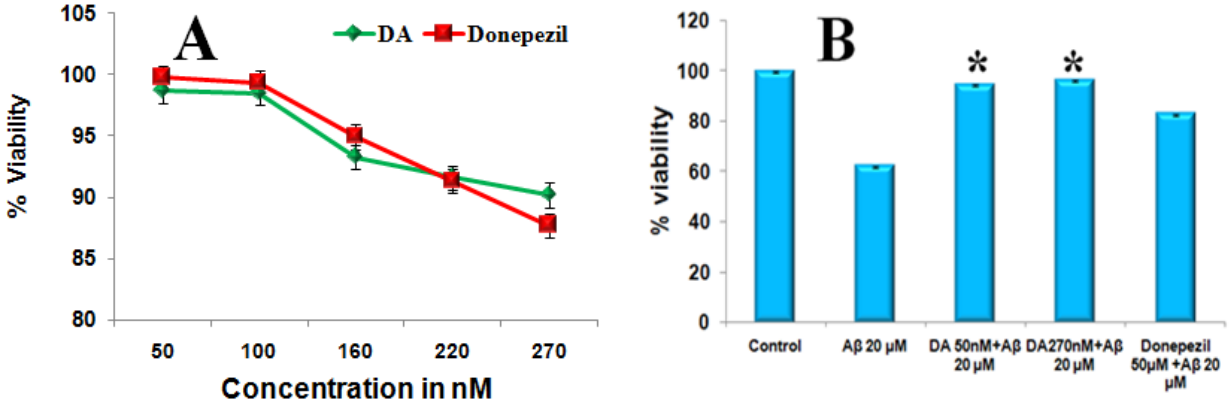

Fig. 7 (A) Effect of different concentrations of DA on viability of N2a cells when compared to the standard drug donepezil, (B) Effect of DA and donepezil on $A\beta_{25-35}$ treated N2a cell viability. *Significant level at $p<0.05$ ($A\beta_{25-35}$ treated versus $A\beta_{25-35}$ and DA treated)

Viability of the cells was further supported by its antioxidant properties or ROS quenching ability where it significantly decreased DCF-DA fluorescence intensity of $A\beta_{25-35}$ treated N2a cells (**Fig. 8)**. The increased cell viability associated with DA treatment against $A\beta_{25-35}$ induced neuronal cell death might be due to its free radical scavenging and potent Aβ anti aggregation ability which might interrupt with the downstream signalling pathways associated with these processes. DA showed significant increase in PBMC viability in a concentration dependent manner up to 24 hr when compared to the positive control which showed 57% decrease in cell viability **(Figure 9)**. **Figure 10** showed hemolytic activity of DA. The result of hemolytic activity rendered low hemolytic activity ranging from 2.35 to 5.61% for 50 to 270nM relative to standard 1% SDS with that of 100%, as positive control. It is thus attributed that the synthesized DA did not damage erythrocyte membrane.

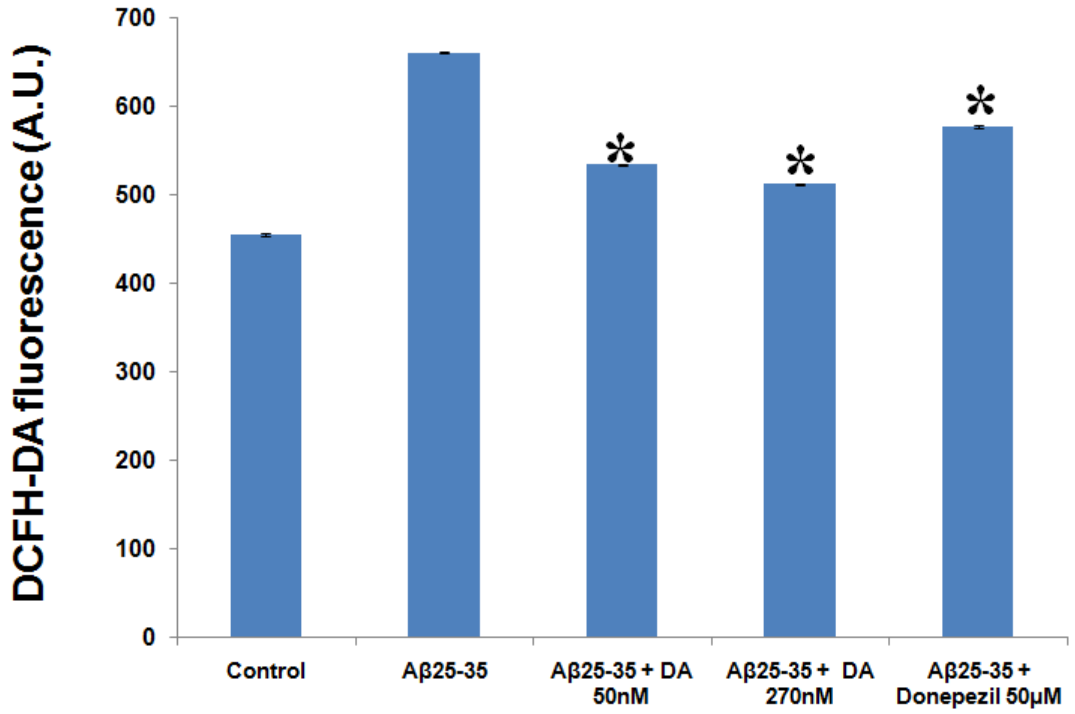

Fig. 8 Effect of DA on ROS production in $A\beta_{25-35}$ treated N2a cells. (*Significant level at $p<0.05$ $A\beta_{25-35}$ treated versus $A\beta_{25-35}$ and DA treated)

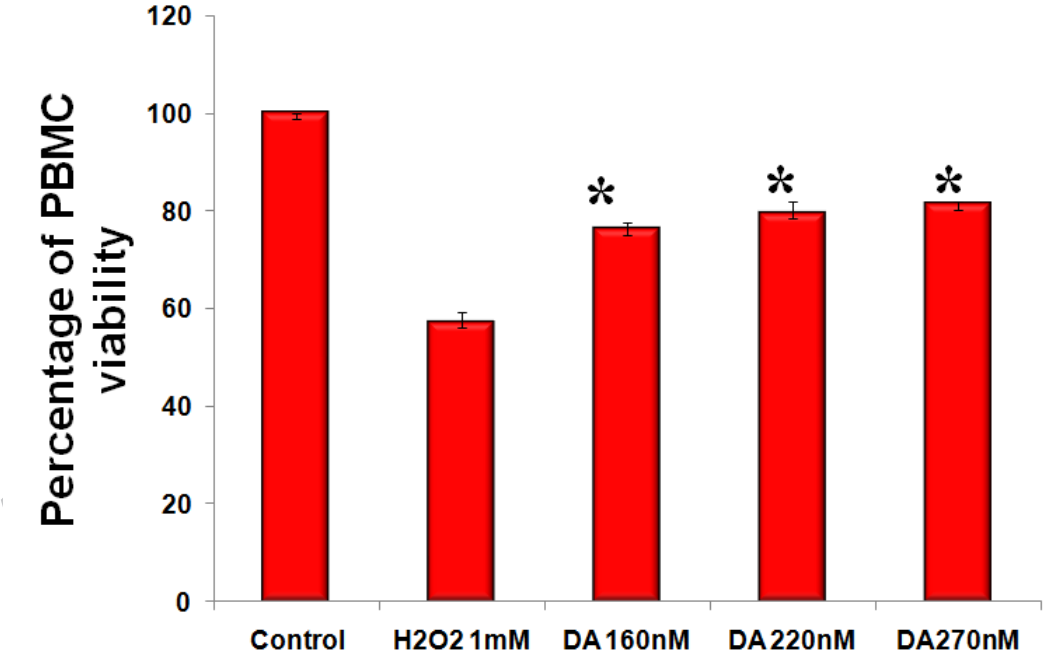

Fig. 9 Cytotoxicity of DA against PBMC at 24 hr compared to that of 1mM H_2O_2. (*Significant level at $p<0.05$ H_2O_2 treated versus DA treated)

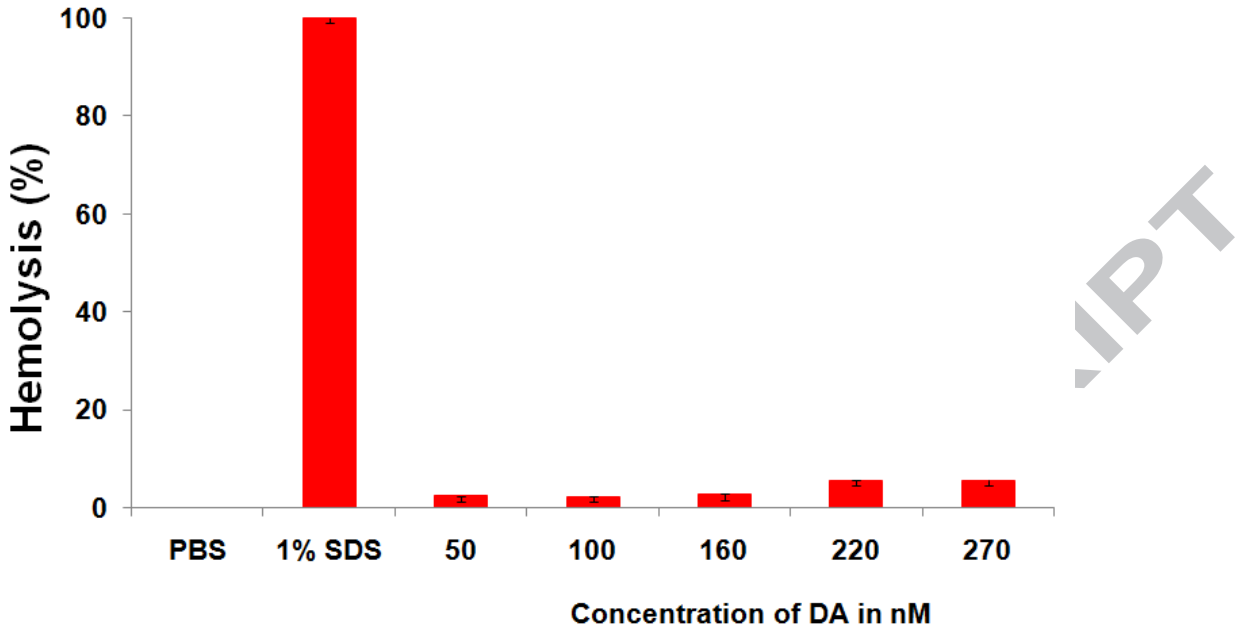

Fig. 10 Hemolysis activity of DA compared to that of 1% SDS.

Further more than 50% of drug candidates fail in clinical trials in the late-stage of AD due to their poor ADME (absorption, distribution, metabolism, and excretion) properties which significantly escalate the cost of new drug development. Therefore we determined the ADME properties for DA using Schrodinger QikProp module to validate its pharmacological profile. Predicted polarizability, predicted hexadecane/gas partition coefficient, predicted octanol/gas partition coefficient, predicted water/gas partition coefficient, predicted octanol/water partition coefficient, predicted aqueous solubility, predicted aqueous solubility, Caco-2 permeability, predicted brain/blood partition coefficient, predicted skin permeability, number of likely metabolic reactions, binding to human serum albumin, predicted qualitative human oral absorption, predicted human absorption on percentage scale, number of violation of Lipinski's rule of five [49] and number of violation of Jorgensen's rule of three [50] were determined and shown in **Table 1**. Interestingly all the predicted values depicted its suitability as a drug candidate. Again principle descriptor values like molecular weight, total solvent accessible

surface area, hydrophobic component of solvent accessible surface area, Pi component of solvent accessible surface area, weakly polar component of the solvent accessible surface area, total solvent-accessible volume in, number of hydrogen bonds that would be donated by the solute to water molecule in an aqueous solution, number of hydrogen bonds that would be accepted by the solute from water molecule in an aqueous solution and globularity descriptor were also in agreement with ADME prediction.

Table 1 Predicted ADME properties of DA

QikProp predicted ADME properties with normal range	QikProp predicted values
Polrz (<70)	20.26
Log PC16 (<18)	5.38
Log Poct (<35)	8.58
Log Pw (4-45)	4.24
Log Po/w (-2.5 to 6.5)	1.57
LogS (-6.5 to 0.5)	-1.98
CI logS (-6.5 to 0.5)	-1.72
PCaco (25 to >500)	2174.55
Log BB (-3 to 1.2)	-1.72
Log Kp (-8 to -1)	-2.71
Metab (1 to 8)	0
Log Khsa (1.5 to 1.5)	-0.28
HOA (1 L, 2M, 3H)	3
PHOA (25 to >80%)	95.88
Rule Of 5 < 4)	0
Rule Of 3 (<3)	0

Predicted polarizability (in Å3) (PolrZ), predicted hexadecane/gas partition coefficient (Log PC16), predicted octanol/gas partition coefficient (Log Poct), predicted water/gas partition coefficient (Log Pw), predicted octanol/water partition coefficient (Log Po/W), predicted aqueous solubility (Log S), conformation independent predicted aqueous solubility (CI logS), Caco-2 permeability in nm sec-1 (PCaco), predicted brain/blood partition coefficient (Log BB), predicted skin permeability (Log Kp), number of likely metabolic reaction (Metab), binding to human serum albumin (Log Khsa), predicted qualitative human oral absorption (HOA), predicted human absorption on percentage scale (PHOA), number of violation of Lipinski's rule of five (Rule of 5) and number of violation of Jorgensen's rule of three (Rule of 3)

Table 2 Principle drug characteristic prediction by QikProp and SwissADME

QikProp predicted Principle drug characteristic properties with normal range	QikProp predicted values
MW (130/750)	180.24
SASA (300/1000)	387.26
FOSA (0/750)	294.00
PISA (0/450)	23.81
WPSA (0/175)	0
M. Vol. (500/2000)	654.542
Donor HB (0/6)	0
Accpt HB (2-20)	3
Glob (0.75/0.95)	0.941
CytP450 inhibitior	No

Molecular weight (mol MW), total solvent accessible surface area (SASA) in $Å^2$, hydrophobic component of SASA (FOSA), Pi (carbon and attached hydrogen) component of SASA (PISA), weakly polar component of the SASA (halogen, P and S) (WPSA), total solvent-accessible volume in Å3 using a probe with a 1.4 Å radius (Molecular volume), number of hydrogen bonds that would be donated by the solute to water molecule in an aqueous solution (Donor HB), number of hydrogen bonds that would be accepted by the solute from water molecule in an aqueous solution (accpt HB) and globularity descriptor (glob).

Further it was not identified as a CytP450 inhibitor **(Table 2)**. These results revealed that DA posses optimal ADME properties and act as a potent cell free AChE inhibitor, free radical scavenger, $A\beta_{25-35}$ antiaggregator and dis aggregator, along with potential cellular ROS

scavenger, at the same time it neither reduce N2a cell viability nor damage erythrocyte membrane. Thus it may mediate its neuroprotective effect *in vitro* and *in vivo* through its multiple therapeutic effects and help to encounter AD condition in a better way.

4. Conclusion

In summary, this study puts light on synthesized DA and its multifunctional anti-Alzheimer potential. DA synthesized from β-ionone was found to be a potent AChE inhibitor with IC_{50} 34.03 nM which was supported by molecular docking studies. It also showed persuasive radical scavenging ability with DPPH, (.NO) scavenging activity and metal chelating activity having IC_{50} value 50nM and >270nM respectively. Significant anti-$A\beta_{25-35}$ aggregation and dis aggregation potency of the compound was observed at 270nM. It significantly prevented amyloid β_{25-35} self-aggregation and promoted its disaggregation at 270nM. It was the first report to be not cytotoxic towards N2a cells up to 24 hr treatment at the same time it significantly increased viability of amyloid β_{25-35} treated N2a cells and reduced amyloid β_{25-35} induced ROS generation at both 50 and 270nM. It's cytotoxic and hemolysis profiles were found to be safe. Drug like properties of DA were also proven using the theoretical ADME analysis. The multitargeted profile of DA elucidated that DA can be considered as a very capable lead compound for anti-AD therapy which can be further extended to study its molecular mechanism.

Conflict of Interest

The authors declare that the research was conducted in the absence of any commercial or financial relationships that could be construed as a potential conflict of interest.

Author Contributions

KPD: supervised the research project; SP and PM: synthesized the compound; MD and NT performed *in vitro* and cell line studies and CN and SKS assisted in ADME, molecular docking and simulation.

Acknowledgements

The authors MD, NT and KPD sincerely acknowledge the computational and bioinformatics facility provided by the Alagappa University Bioinformatics Infrastructure Facility (funded by DBT, GOI; File No. BT/BI/25/012/2012,BIF). The authors also thankfully acknowledge DST-FIST (Grant No. SR/FST/LSI-639/2015(C)), UGC-SAP (Grant No. F.5-1/2018/DRS-II(SAP-II)) and DST-PURSE (Grant No. SR/PURSE Phase 2/38 (G)) for providing instrumentation facilities. The author MD wishes to thank DST-PURSE (No. SR/PURSE Phase 2/38 (G), 21/02/2017) for the Junior Research Fellowship. SP is thankful to University Grants Commission (UGC), New Delhi, for providing Post Doctoral Research Fellowship (201516-PDFSS-2015-17-TAM-10968).

Abbreviations

AChE- Acetylcholinesterase

AChEI- Acetylcholinesterase Inhibitors

AD- Alzheimer's disease

ADME- Absorption Distribution Metabolism Excretion

NO- Nitric Oxide

DA- Dihydroactinidiolide

DPPH - 2,2-diphenyl-1-picrylhydrazyl

RMSD- Root Mean Square Deviation

NFTs-Neurofibrillary tangles

MTDLs- Multi-target directed ligands

ThT- Thioflavin T

DTNB- 5,5-dithio-bis-(2-nitrobenzoic acid)

Notes and References

[1] Klok, J., Baas, M., Cox, H. C., De Leeuw, J. W., Schenck, P. A. (1984). Loliolides and dihydroactinidiolide in a recent marine sediment probably indicate a major transformation pathway of carotenoids. Tetrahedron Letters, 25(48), 5577-5580

[2] Dinis, T. C., Madeira, V. M., Almeida, L. M. (1994). Action of phenolic derivatives (acetaminophen, salicylate, and 5-aminosalicylate) as inhibitors of membrane lipid peroxidation and as peroxyl radical scavengers. Archives of Biochemistry and Biophysics, 315(1), 161-169

[3] Borse, B. B., Rao, L. J. M., Nagalakshmi, S., Krishnamurthy, N. (2002). Fingerprint of black teas from India: identification of the regio-specific characteristics. Food Chemistry, 79(4), 419-424

[4] Huang, L. F., Zhong, K. J., Sun, X. J., Wu, M. J., Huang, K. L., Liang, Y. Z., Guo, F.Q., Li, Y. W. (2006). Comparative analysis of the volatile components in cut tobacco from different locations with gas chromatography–mass spectrometry (GC–MS) and combined chemometric methods. Analytica Chimica acta, 575(2), 236-245

[5] Stevens, K. L., Merrill, G.B. (1981) Dihydroactinidiolide—a potent growth inhibitor from *Eleocharis coloradoensis* (spikerush). Cellular and Molecular Life Sciences, 37(11):1133

[6] Shumbe, L., Bott, R., Havaux, M. (2014) Dihydroactinidiolide, a high light-induced β-carotene derivative that can regulate gene expression and photoacclimation in Arabidopsis. Molecular Plant, 7(7):1248-1251

[7] Rocca, J. R., Tumlinson, J. H. Glancey, B. M, Lofgren, C. S. (1983) Synthesis and stereochemistry of tetrahydro-3, 5-dimethyl-6-(1) methylbutyl)-2H-pyran-2-one, a

component of the queen recognition pheromone of *Solenopsis invicta*. Tetrahedron Letter, 24(18):1893-1896

[8] Isoe, S. (1995) Progress in the synthesis of iridoids and related natural products. In Studies in Natural Products Chemistry (Vol. 16, pp. 289-320). Elsevier.

[9] Saad, A.M., Ghareeb, M.A., Abdel-Aziz, M.S., Madkour, H.M., Khalaf, O.M., El-Ziaty, A.K., Abdel-Mogib, M. (2017) Chemical constituents and biological activities of different solvent extracts of *Prosopis farcta* growing in Egypt. Journal of Pharmacology and Phytotherapy, 9(5):67-76

[10] Laungsuwon, R., Chulalaksananukul, W. (2014) Chemical composition and antibacterial activity of extracts from freshwater green algae, *Cladophora glomerata* Kützing and *Microspora floccosa* (Vaucher) Thuret. Journal of BioScience and Biotechnology, 1;3(3)

[11] Mori, K., Nakazono, Y. (1986) Synthesis of both the enantiomers of dihydroactinidiolide. a pheromone component of the red imported fire ant. Tetrahedron, 42(1):283-290

[12] Chakraborty, T. K., Chandrasekaran, S. (1984). A facile entry to bicyclic γ-lactones and a short synthesis of (±)-dihydroactinidiolide. Tetrahedron Letters, 25(27), 2895-2896

[13] Cain, C. M., Simpkins, N. S. (1987). Concise asymmetric synthesis of (5S, 6S)-aeginetolide and (5S)-dihydroactinidiolide. Tetrahedron Letters, 28(32), 3723-3724

[14] Mori, K., Khlebnikov, V. (1993). Carotenoids and Degraded Carotenoids, VIII– Synthesis of (+)-Dihydroactinidiolide,(+)-and (−)-Actinidiolide,(+)-and (−)-Loliolide as well as (+)-and (−)-Epiloliolide. Liebigs Annalen der Chemie, 1993 (1), 77-82

[15] Subbaraju GV, Manhas MS, Bose AK (1991) An improved synthesis of (±)-dihydroactinidiolide. Tetrahedron Letter, 32(37):4871-4874

[16] Eidman, K. F., MacDougall, B. S. (2006). Synthesis of loliolide, actinidiolide, dihydroactinidiolide, and aeginetolide via cerium enolate chemistry. The Journal of Organic Chemistry, 71(25), 9513-9516

[17] Bosser, A., Paplorey, E., Belin, J. M. (1995). A Simple Way to (±)-Dihydroactinidiolide from β-Ionone Related to the Enzymic Co-oxidation of β-Carotene in Aqueous Solution. Biotechnology Progress, 11(6), 689-692

[18] Dabdoub, M. J., Silveira, C. C., Lenardão, E. J., Guerrero Jr, P. G., Viana, L. H., Kawasoko, C. Y., Baroni, A. C. (2009). Total synthesis of (±)-dihydroactinidiolide using selenium-stabilized carbenium ion. Tetrahedron Letters, 50(40), 5569-5571

[19] Lu, C., Zhou, Q., Yan, J., Du, Z., Huang, L., Li, X. (2013). A novel series of tacrine–selegiline hybrids with cholinesterase and monoamine oxidase inhibition activities for the treatment of Alzheimer's disease. European Journal of Medicinal Chemistry, 62, 745-753

[20] Small, D. H. (2005) Acetylcholinesterase inhibitors for the treatment of dementia in Alzheimer's disease: do we need new inhibitors?. Expert Opinion Emerging Drugs 10(4):817-825

[21] Youdim, M. B., Buccafusco, J. J. (2005) Multi-functional drugs for various CNS targets in the treatment of neurodegenerative disorders. Trends Pharmacological Science 26(1):27-35

[22] Cappelli, A., Gallelli, A., Manini, M., Anzini, M., Mennuni, L., Makovec, F., Menziani, M. C., Alcaro, S., Ortuso, F., Vomero, S. (2005). Further studies on the interaction of the 5-hydroxytryptamine3 (5-HT3) receptor with arylpiperazine ligands. Development

of a new 5-HT3 receptor ligand showing potent acetylcholinesterase inhibitory properties. Journal of Medicinal Chemistry, 48(10), 3564-3575

[23] Kumar, D., Gupta, S. K., Ganeshpurkar, A., Gutti, G., Krishnamurthy, S., Modi, G., Singh, S. K. (2018). Development of Piperazinediones as dual inhibitor for treatment of Alzheimer's disease. European Journal of Medicinal Chemistry, 150, 87-101

[24] Hansen, R. A., Gartlehner, G., Webb, A. P., Morgan, L. C., Moore, C. G., Jonas, D. E. (2008). Efficacy and safety of donepezil, galantamine, and rivastigmine for the treatment of Alzheimer's disease: a systematic review and meta-analysis. Clinical Interventions in aging, 3(2), 211

[25] Knapp, M. J., Knopman, D. S., Solomon, P. R., Pendlebury, W. W., Davis, C. S., Gracon, S. I., Apter, J. T., Lazarus, C. N., Baker, K.E., Barnett, M., Baumel, B. (1994). A 30-week randomized controlled trial of high-dose tacrine in patients with Alzheimer's disease. Jama, 271(13), 985-991

[26] Sheeja, M. D., Beema, S. R., Karutha, P. S., Pandima, D. K. (2017) Cholinesterase inhibitory, anti-amyloidogenic and neuroprotective effect of the medicinal plant *Grewia tiliaefolia*–An *in vitro* and *in silico* study. Pharmacological Biology, 55(1):381-393

[27] Shanmuganathan B, Pandima, D. K. (2016) Evaluation of the nutritional profile and antioxidant and anti-cholinesterase activities of *Padina gymnospora* (Phaeophyceae). European Journal Phycology, 51(4):482-490

[28] Zeng Y, Li Y, Yang J, Pu X, Du J, Yang X, Yang T, Yang S (2017) Therapeutic role of functional components in Alliums for preventive chronic disease in human being. Evid Based Complement Alternat Med

[29] Nwidu, L.L., Elmorsy, E., Thornton, J., Wijamunige, B., Wijesekara, A., Tarbox, R., Warren, A., Carter, W. G. (2017) Anti-acetylcholinesterase activity and antioxidant properties of extracts and fractions of *Carpolobia lutea*. Pharmaceutical Biology, 55(1):1875-1883

[30] Ingale, S. P., Kasture, S. B. (2017). Protective Effect of Standardized Extract of Passiflora incarnata Flower in Parkinson's and Alzheimer 's disease. Ancient Science of Life, 36(4), 200

[31] Chaudhari, K. S., Tiwari, N. R., Tiwari, R. R., Sharma, R. S. (2017). Neurocognitive Effect of Nootropic Drug Brahmi (*Bacopa monnieri*) in Alzheimer's disease. Annals of neurosciences, 24(2), 111-122

[32] Sachihiko, I., Suong, B. H., Hiroshi, I., Shigeo, K., Takeo, S. (1968) The synthesis of actinidiolide, dihydroactinidiolide and actinidol. Tetrahedron Letter, 9(53):5561-5564

[33] Ellman, G. L., Courtney, K. D., Andres Jr, V., Featherstone, R. M. (1961). A new and rapid colorimetric determination of acetylcholinesterase activity. Biochemical Pharmacology, 7(2), 88-95

[34] Blois, M. S. (1958). Antioxidant determinations by the use of a stable free radical. Nature, 181(4617), 1199.

[35] Griess, P. (1879). Comments on the essay of HH Weselsky and Benedict 'About some azo compounds'. Chemische Berichte, 12, 426-428

[36] Dinis, T. C., Madeira, V. M., Almeida, L. M. (1994). Action of phenolic derivatives (acetaminophen, salicylate, and 5-aminosalicylate) as inhibitors of membrane lipid peroxidation and as peroxyl radical scavengers. Archives of Biochemistry and Biophysics, 315(1), 161-169

[37] Munoz-Ruiz, P., Rubio, L., García-Palomero, E., Dorronsoro, I., del Monte-Millán, M., Valenzuela, R., Usán, P., de Austria, C., Bartolini, M., Andrisano, V., Bidon-Chanal, A. (2005) Design, synthesis, and biological evaluation of dual binding site acetylcholinesterase inhibitors: new disease-modifying agents for Alzheimer's disease. Journal of Medicinal Chemistry, 48(23):7223-7233

[38] Parnham, M.J., Wetzig, H. (1993) Toxicity screening of liposomes. Chemistry and Physics of Lipids, 64(1-3):263-274

[39] Zhou, B., Zhang, B., Li, X., Liu, X., Li, H., Li, D., Cui, Z., Geng, H., Zhou, L. (2018) New 2-Aryl-9-methyl-β-carbolinium salts as Potential Acetylcholinesterase Inhibitor agents: Synthesis, Bioactivity and Structure–Activity Relationship. Scientific Reports, 8(1):1559

[40] Wu, G., Gao, Y., Kang, D., Huang, B., Huo, Z., Liu, H., Poongavanam, V., Zhan, P., Liu, X. (2018) Design, synthesis and biological evaluation of tacrine-1, 2, 3-triazole derivatives as potent cholinesterase inhibitors. Medicinal Chemistry Communications, 9:149-159

[41] Sepsova V, Karasova JZ, Korabecny J, Dolezal R, Zemek F, Bennion BJ, Kuca K (2013) Oximes: inhibitors of human recombinant acetylcholinesterase. A structure-activity relationship (SAR) study. International Journal of Molecular Science, 14(8):16882-16900

[42] Giarman, N.J., Schmidt, K.F. (1963) Some neurochemical aspects of the depressant action of γ-butyrolactone on the central nervous system. British Journal of Pharmacological Chemotherapy, 20(3):563-568

[43] Shrivastava, S. K., Srivastava, P., Upendra, T.V., Tripathi, P.N., Sinha, S.K. (2017) Design, synthesis and evaluation of some N-methylenebenzenamine derivatives as selective acetylcholinesterase (AChE) inhibitor and antioxidant to enhance learning and memory. Bioorganic Medicinal Chemistry 25(4):1471-1480

[44] Jiang, Z., Chen, Y., Yao, F., Chen, W., Zhong, S., Zheng, F., Shi, G. (2013). Antioxidant, antibacterial and antischistosomal activities of extracts from *Grateloupia livida* (Harv). Yamada. PloS one, 8(11), e80413

[45] Sens, L., de Oliveira, A. S., Mascarello, A., Brighente, I. M., Yunesa, R. A., Nunesa, R. J. (2018) Synthesis, Antioxidant Activity, Acetylcholinesterase Inhibition and Quantum Studies of Thiosemicarbazones. Journal of Brazilian Chemical Society 29(2):343-352

[46] Clementi, M. E., Marini, S., Coletta, M., Orsini, F., Giardina, B., Misiti, F. (2005). Aβ (31–35) and Aβ (25–35) fragments of amyloid beta-protein induce cellular death through apoptotic signals: Role of the redox state of methionine-35. FEBS Letters, 579(13), 2913-2918

[47] Chauhan, A., Ray, I., Chauhan, V. P. (2000). Interaction of amyloid beta-protein with anionic phospholipids: possible involvement of Lys28 and C-terminus aliphatic amino acids. Neurochemical Research, 25(3), 423-429

[48] Hernández-Rodríguez, M., Correa-Basurto, J., Benitez-Cardoza, C. G., Resendiz-Albor, A. A., Rosales-Hernández, M. C. (2013). In silico and in vitro studies to elucidate the role of Cu2+ and galanthamine as the limiting step in the amyloid beta (1–42) fibrillation process. Protein Science, 22(10), 1320-1335

[49] Lipinski, C.A. Avoiding investment in doomed drugs. Current Drug Discovery. 2001;1:17-19

[50] Jorgensen, W. L. (2009). Efficient drug lead discovery and optimization. Accounts of chemical research, 42(6), 724-733

Highlights:

- Dihydroactinidiolide had powerful acetylcholinesterase inhibitory activity.
- It had antioxidant and anti aggregation activity compared to the respective standards.
- Dihydroactinidiolide was not cytotoxic towards N2A cells.
- It increased viability of amyloid β treated N2A cells via reduced ROS generation.
- Its ADME and hemolysis profiles were found to be safe.

Graphical abstract